STIM protein coupling in the activation of Orai channels

Youjun Wang[a,1], Xiaoxiang Deng[a,1], Yandong Zhou[a,1], Eunan Hendron[a], Salvatore Mancarella[a], Michael F. Ritchie[a], Xiang D. Tang[b], Yoshihiro Baba[c], Tomohiro Kurosaki[c], Yasuo Mori[d], Jonathan Soboloff[a,2], and Donald L. Gill[a,2]

[a]Department of Biochemistry, Temple University School of Medicine, Philadelphia, PA 19140; [b]Department of Pharmacology, Nankai University School of Medicine, Nankai, Tianjin, China; [c]Laboratory of Lymphocyte Differentiation, WPI Immunology Frontier Research Center, Osaka University, Suita, Osaka 565-0871, Japan; and [d]Laboratory of Molecular Biology, Department of Synthetic Chemistry and Biological Chemistry, Kyoto University, Kyoto 606-8501, Japan

Edited by Solomon H. Snyder, Johns Hopkins University School of Medicine, Baltimore, MD, and approved February 18, 2009 (received for review January 9, 2009)

STIM proteins are sensors of endoplasmic reticulum (ER) luminal Ca^{2+} changes and rapidly translocate into near plasma membrane (PM) junctions to activate Ca^{2+} entry through the Orai family of highly Ca^{2+}-selective "store-operated" channels (SOCs). Dissecting the STIM–Orai coupling process is restricted by the abstruse nature of the ER–PM junctional domain. To overcome this problem, we studied coupling by using STIM chimera and cytoplasmic C-terminal domains of STIM1 and STIM2 (S1ct and S2ct) and identifying a fundamental action of the powerful SOC modifier, 2-aminoethoxydiphenyl borate (2-APB), the mechanism of which has eluded recent scrutiny. We reveal that 2-APB induces profound, rapid, and direct interactions between S1ct or S2ct and Orai1, effecting full Ca^{2+} release-activated Ca^{2+} (CRAC) current activation. The short 235-505 S1ct coiled-coil region was sufficient for functional Orai1 coupling. YFP-tagged S1ct or S2ct fragments cleared from the cytosol seconds after 2-APB addition, binding avidly to Orai1-CFP with a rapid increase in FRET and transiently increasing CRAC current 200-fold above basal levels. Functional S1ct–Orai1 coupling occurred in STIM1/STIM2$^{-/-}$ DT40 chicken B cells, indicating ct fragments operate independently of native STIM proteins. The 2-APB-induced S1ct–Orai1 and S2-ct–Orai1 complexes undergo rapid reorganization into discrete colocalized PM clusters, which remain stable for >100 s, well beyond CRAC activation and subsequent deactivation. In addition to defining 2-APB's action, the locked STIMct–Orai complex provides a potentially useful probe to structurally examine coupling.

calcium signaling | DT40 cells | CRAC channel

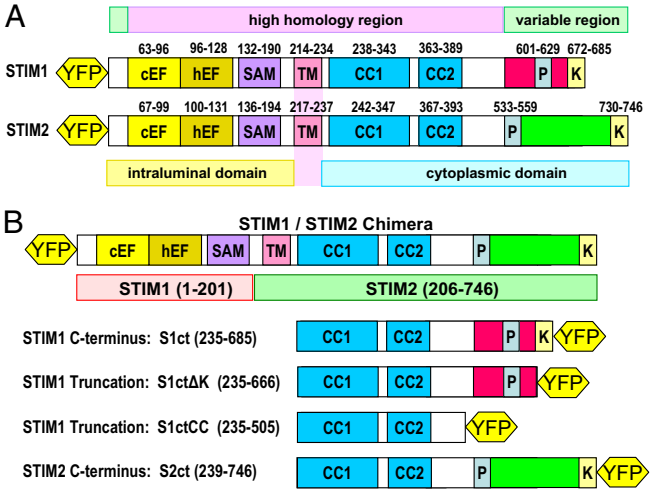

Fig. 1. Schematic illustration of the structures of STIM proteins and constructs used. (*A*) Comparison of the sequence domains of STIM1 and STIM2 proteins including the canonical and the hidden EF-hand Ca^{2+} binding regions (cEF and hEF), sterile-α motifs (SAM), transmembrane domains (TM), 2 coiled-coil regions (CC1 and CC2), proline-rich domains (P), and lysine-rich domains (K). (*B*) Structures of STIM chimera and C-terminal (ct) truncations used in these studies. S1ctΔK is deficient in just the C-terminal lysine-rich domain; S1ctCC is deficient in the entire variable region, and comprises mostly the coiled-coil region of STIM1. All proteins were YFP-tagged as shown.

A dynamic interplay between 2 membrane proteins, STIM and Orai, underlies an intricate coupling between Ca^{2+} release from endoplasmic reticulum (ER) stores and Ca^{2+} entry across the plasma membrane (PM) (1–3). The single spanning transmembrane proteins STIM1 and STIM2 function as sensors of ER luminal Ca^{2+} changes (4–7). Depletion of luminal Ca^{2+} within ER stores triggers STIM proteins to aggregate and undergo rapid translocation into closely juxtaposed ER–PM junctions to activate Ca^{2+} entry through one or more of the 3-member family of PM tetra-spanning channel proteins, Orai1, Orai2, and Orai3 (8–10). The Orai proteins function as highly Ca^{2+}-selective "store-operated" channels (SOCs) (11, 12). The activation of SOCs is crucial in mediating longer-term cytosolic Ca^{2+} signals, replenishing intracellular stores, and homeostatic control of both cytosolic and ER luminal Ca^{2+} levels (3, 11–14). Orai1 coexpressed with STIM1 reconstitutes high levels of the inwardly-rectifying Ca^{2+} release-activated Ca^{2+} (CRAC) current (10, 15–17), the hallmark of SOCs (11, 12).

Despite close interactions (5, 18), the coupling mechanism between STIM and Orai proteins to activate Ca^{2+} entry remains to be elucidated. Our approach was to examine the STIM–Orai interactions by using the reactive borate 2-aminoethoxydiphenyl borate (2-APB), a powerful modifier of SOC function (11, 19–21). Its actions are complex, enhancing SOC activation at 5–10 μM, yet blocking it at 50 μM (20, 21). Recent evidence emphasizes the remarkable effectiveness and the complexities of 2-APB in modifying STIM protein function and Orai channel gating (22–25). Although its actions are enigmatic, they indicate 2-APB is a valuable tool in deciphering the STIM–Orai coupling mechanism. Our studies reveal that 2-APB induces profound, rapid, and direct interactions between C-terminal fragments of STIM1 or STIM2 and the Orai1 protein, resulting in full CRAC current activation. The 2-APB-induced C-terminal STIM–Orai complexes undergo rapid reorganization into discrete clusters within the PM. The studies not only define the action of 2-APB in mediating STIM–

Author contributions: Y.W., X.D., Y.Z., E.H., M.F.R., T.K., J.S., and D.L.G. designed research; Y.W., X.D., Y.Z., E.H., S.M., M.F.R., and X.D.T. performed research; Y.B., T.K., and Y.M. contributed new reagents/analytic tools; Y.W., X.D., Y.Z., E.H., S.M., M.F.R., X.D.T., J.S., and D.L.G. analyzed data; and Y.W., X.D., Y.Z., J.S., and D.L.G. wrote the paper.

The authors declare no conflict of interest.

This article is a PNAS Direct Submission.

[1]Y.W., X.D., and Y.Z. contributed equally to this work.

[2]To whom correspondence may be addressed. E-mail: dgill@temple.edu or soboloff@temple.edu.

This article contains supporting information online at www.pnas.org/cgi/content/full/0811818106/DCSupplemental.

BIOCHEMISTRY

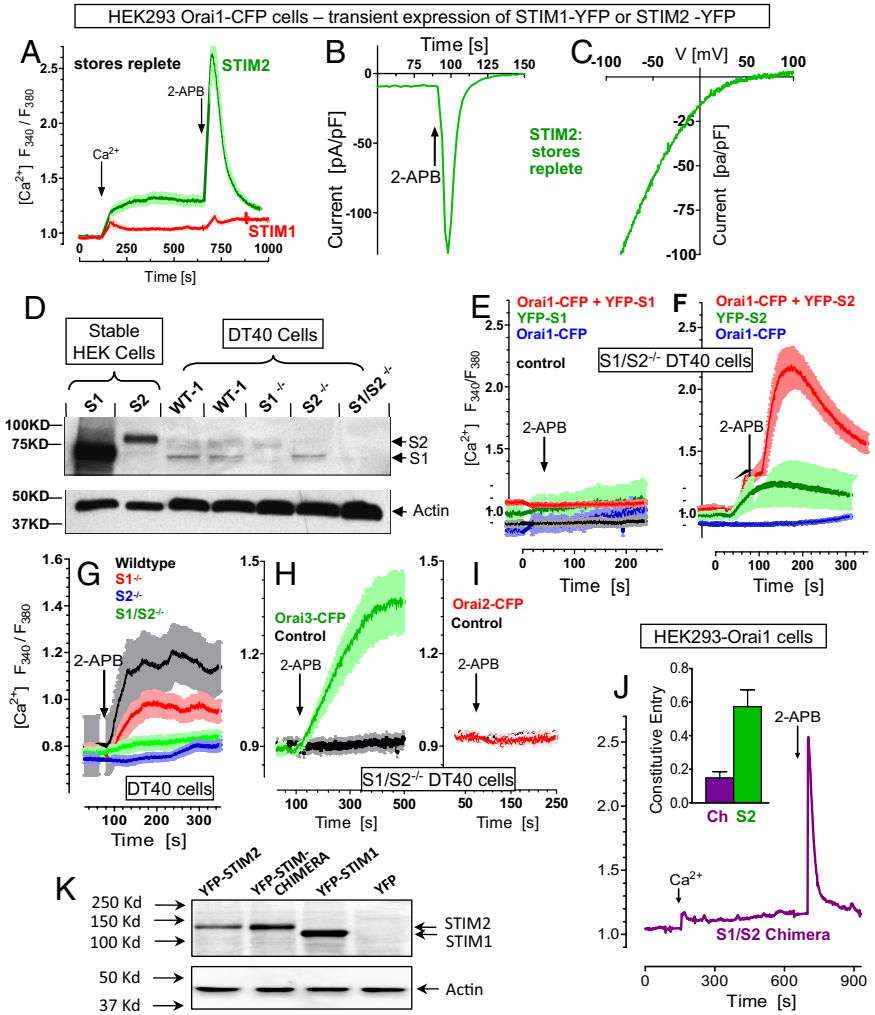

Fig. 2. Distinct actions of STIM1 and STIM2 in coupling to activate Orai channels. (*A*) Cytosolic Ca^{2+} responses were measured in HEK293 cells stably expressing Orai1–CFP (HEK–Orai1), with either STIM1–YFP (red) and STIM2–YFP (green) transiently transfected. Ca^{2+} (1 mM) or 50 μM 2-APB were added as shown (arrows). (*B*) Time course of typical whole-cell current measurement in 10 mM Ca^{2+} in HEK–Orai1 cells transfected with STIM2 (−100 mV holding potential); 50 μM 2-APB was added as shown. (*C*) *I–V* curve showing typical CRAC channel properties of STIM2-mediated peak current in HEK–Orai1 cells transfected with STIM2. (*D*) Western analysis using STIM1/STIM2 cross-reacting mAb revealing STIM1 (S1) and STIM2 (S2) expression in either of 2 WT DT40 cell lines (WT-1 and WT-2), or either $S1^{-/-}$, $S2^{-/-}$, or $S1/S2^{-/-}$ DT40 KO cells. HEK293 cells expressing either S1 or S2 were used as positive controls, and actin was used as loading control. (*E*) Ca^{2+} responses to 50 μM 2-APB in 1 mM Ca^{2+} in $S1/S2^{-/-}$ DT40 cells transfected either with empty pIRES vector (black), Orai1–CFP (blue), YFP–STIM1 (green), or both Orai1–CFP and YFP–STIM1 (red). (*F*) Ca^{2+} responses to 50 μM 2-APB in 1 mM Ca^{2+} in $S1/S2^{-/-}$ DT40 cells transfected either with Orai1–CFP (blue), YFP–STIM2 (green), or both Orai1–CFP and YFP–STIM2 (red). (*G*) Effects of 50 μM 2-APB on Ca^{2+} responses in 1 mM Ca^{2+} in either WT DT40 cells (black) or $S1^{-/-}$ DT40 cells (red), $S2^{-/-}$ DT40 cells (blue), or $S1/S2^{-/-}$ DT40 cells (green). (*H*) Effects of 50 μM 2-APB on Ca^{2+} entry (1 mM) in $S1S2^{-/-}$ DT40 cells expressing either empty pIRES vector (black) or expressing Orai3–CFP (green). (*I*) Effects of 50 μM 2-APB on Ca^{2+} entry (1 mM) in $S1S2^{-/-}$ DT40 cells expressing either empty pIRES vector (black) or Orai2–CFP (red). (*J*) Ca^{2+} responses in HEK–Orai1 cells expressing the STIM1/STIM2 chimera (see Fig. 1); 50 μM 2-APB or 1 mM Ca^{2+} were added as shown. (*Inset*) Average constitutive Ca^{2+} entry in HEK-Orai1 cells transfected either with STIM2 (green) or the YFP-STIM1/STIM2 chimera (purple); means ± SEM, 5 experiments (10–40 cells each). (*K*) Western analysis of chimeric YFP–STIM1/STIM2 expression in HEK–Orai cells using anti-YFP antibody and comparison of expression with YFP–STIM1 and YFP–STIM2.

Orai interactions, but also suggest that the 2-APB-induced avid coupling between STIM and Orai proteins may be a useful means to structurally examine the interacting sites.

Results and Discussion

Although STIM1 and STIM2 have similar structures (Fig. 1*A*), we noted some perplexing distinctions in the actions of 2-APB on each protein (16, 26). As shown in Fig. 2*A*, using HEK293 cells stably overexpressing Orai1–CFP (HEK-Orai1), the coexpression of YFP–STIM2 resulted in increased constitutive entry of Ca^{2+} and a massive increase in Ca^{2+} entry upon the addition of 50 μM 2-APB, despite stores remaining full. In contrast, cells coexpressing similar levels of YFP–STIM1 showed little constitutive and almost no 2-APB-induced Ca^{2+} entry. In store-replete STIM2-expressing HEK–Orai1 cells, there was a constitutive current of ≈8 pA/pF, which became activated by 2-APB peaking as high as 100 pA/pF (Fig. 2*B*). The massive current represents authentic CRAC channel activity as revealed from the typical inwardly rectifying current–voltage relationship (Fig. 2*C*). This level of I_{CRAC} is some 200-fold higher than maximal I_{CRAC} in untransfected HEK293 cells (≈0.5 pA/pF). This huge current activation was similar in magnitude to that observed in response to store-depletion in HEK–Orai1 cells coexpressing STIM1 (16). However, in contrast, added after attainment of maximal I_{CRAC}, 50 μM 2-APB completely inhibits the STIM1-mediated current after a very transient activation as described (6, 16, 20).

Why would 2-APB induce such profoundly different effects on STIM1 vs. STIM2? We examined the actions of 2-APB further in DT40 chicken B cells lacking both STIM protein genes to provide a background devoid of endogenous STIM proteins. Western analysis of the relative levels of STIM proteins in cells devoid of STIM1 ($S1^{-/-}$), STIM2 ($S2^{-/-}$), or both STIM1 and STIM2 ($S1/S2^{-/-}$) revealed no obvious compensatory expression (Fig. 2*D*). In these cells coexpression of Orai1–CFP and YFP–STIM1 resulted in no direct activation by 2-APB (Fig. 2*E*). In contrast, expression of STIM2–YFP alone resulted in significant 2-APB-induced Ca^{2+} entry and, coexpressed with Orai1-CFP, resulted in very large Ca^{2+} entry (Fig. 2*F*). We also examined the role of endogenous STIM protein expression by comparing WT DT40 cells with those deficient in either or both of the 2 STIM proteins. 2-APB induced modest Ca^{2+} entry in WT DT40 cells (Fig. 2*G*) that was reduced slightly in STIM1 KO cells ($S1^{-/-}$). In STIM2 KO cells ($S2^{-/-}$), 2-APB induced almost no effect, similar to that observed in the double KO cells.

These results revealed that the 2-APB-induced Ca^{2+} entry was exclusively mediated by STIM2. The action of 2-APB on SOCs is complex; recent studies suggest 2-APB may directly activate Orai3 channels (22–25), an effect thought to be independent of STIM1. We determined that the avian genome is missing the Orai3 gene (only Orai1 and Orai2 are expressed in DT40 cells), hence the profound stimulatory actions of STIM2 on Ca^{2+} entry do not reflect any Orai3 role. Significantly, although the recent Orai3 studies claimed 2-APB activated independently of STIM1, the role

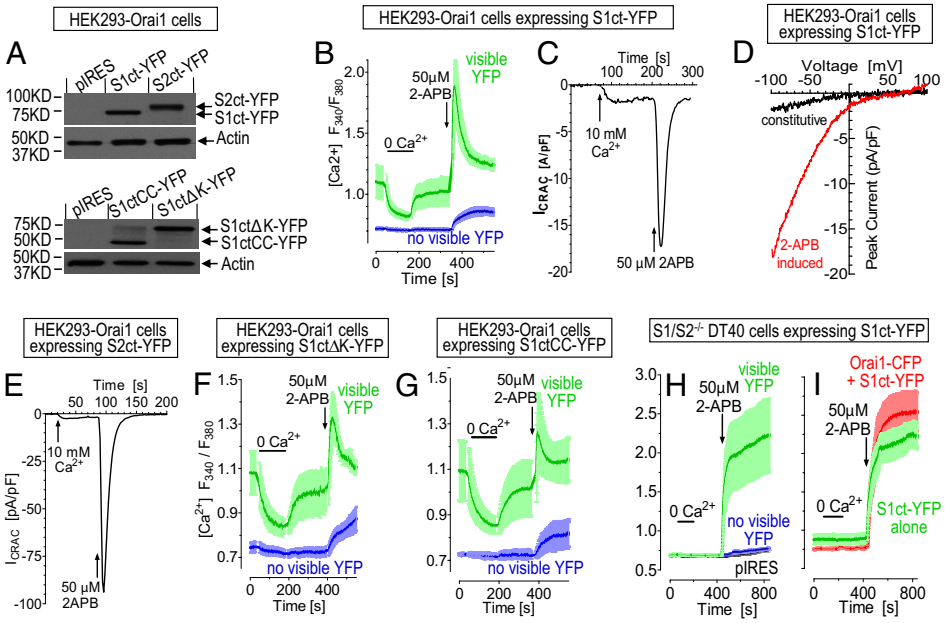

Fig. 3. Functional comparison of STIM1 and STIM2 C-terminal constructs on Orai1 channel activation. Descriptions of constructs are given in Fig. 1*B*. (*A*) Western analysis of expression levels of truncated STIM constructs using a YFP mAb in HEK–Orai1 cells; actin was the loading control. (*B*) Cytosolic Ca^{2+} responses in HEK–Orai1 cells expressing the YFP-tagged C terminus of STIM1 (S1ct–YFP). Cells with visible YFP fluorescence (green) are compared with cells in which YFP was not detectable (blue). Responses in cells with no visible YFP fluorescence reflect low levels of S1ct expression. Measurements were in 1 mM Ca^{2+} except where decreased to 0 (bar); 50 μM 2-APB was added as shown. (*C*) Time course of whole-cell current at −100 mV in a typical HEK–Orai1 cell transfected with S1ct–YFP. (*D*) *I–V* curve of constitutive (black) and 2-APB-induced peak current (red) of the cell shown in *C*. (*E*) Time course of whole-cell current at −100 mV in a HEK–Orai1 cell transfected with S2ct–YFP with similar fluorescence level as cell shown in C. (*F*) Cytosolic Ca^{2+} responses in HEK–Orai1 cells expressing the S1ctΔK-YFP (see Fig. 1). Cells with visible YFP are green; cells without visible YFP are blue. External Ca^{2+} was 1 mM and decreased to 0 (bar); 50 μM 2-APB was added as shown. (*G*) Cytosolic Ca^{2+} responses in HEK–Orai1 cells expressing the S1ctCC–YFP (see Fig. 1) measured exactly as in *F*. (*H*) Effects of S1ct–YFP expression on cytosolic Ca^{2+} responses in S1/S2$^{-/-}$DT40 cells. Cells with visible YFP are green; cells without visible YFP are blue; cells expressing only pIRES vectors are black. External Ca^{2+} was 4 mM and decreased to 0 (bar); 50 μM 2-APB was added as shown. (*I*) Comparison of S1ct–YFP expression with coexpression of S1ct–YFP together with Orai1–CFP in S1/S2$^{-/-}$DT40 cells. Responses were as in *H* except only cells with visible fluorescence are shown.

of STIM2 was not addressed. Considering the huge STIM2-mediated Ca^{2+} entry activated by 2-APB, it was crucial to determine the effect of 2-APB on Orai3 in the absence of STIM2. Interestingly, 2-APB still induced a large Ca^{2+} increase in DT40 S1/S2$^{-/-}$ cells transfected with Orai3–CFP (Fig. 2*H*), providing unequivocal proof that 2-APB activates Orai3 independently of any STIM protein involvement. In contrast to Orai3, Orai2–CFP expressed in S1/S2$^{-/-}$ cells resulted in no 2-APB activation of Ca^{2+} entry (Fig. 2*I*), consistent with previous reports revealing Orai2 is not directly activated by 2-APB (22, 25).

What differences in the structures of STIM1 and STIM2 could account for the vast differences in 2-APB action? Although the STIM1 and STIM2 sequences are highly homologous in the first 500 amino acids (Fig. 1*A*), there are some important differences. In the first luminal EF-hand Ca^{2+}-binding sequence of STIM1, there are 3 amino acids (A79, N80, and D82) that differ from STIM2, imparting a higher Ca^{2+} affinity for STIM1 (13, 27, 28). STIM2, with an increased sensitivity to luminal Ca^{2+} changes, has the propensity to be more "constitutively" active, being activated by relatively smaller luminal Ca^{2+} changes (13). Indeed, our results revealed more constitutive activation of Ca^{2+} entry by STIM2 (Fig. 2 *A* and *B*). Could the activation by 2-APB also reflect this difference, STIM2 perhaps being "primed" by virtue of its constitutive activation? We examined a YFP–STIM1/STIM2 chimera comprising the STIM1 EF-hand region and SAM domain (residues 1–201), attached to the remaining STIM2 sequence (residues 206–746), including the TM and entire C-terminal cytoplasmic region of STIM2 (Fig. 1*B*). Transfected into HEK–Orai1 cells, the chimera resulted in a phenotype of just 20% of the constitutive Ca^{2+} entry mediated by STIM2 (Fig. 2*J Inset*), yet retaining a large and rapid 2-APB-induced Ca^{2+} entry (Fig. 2*J*), suggesting the difference in effectiveness of 2-APB on STIM proteins relates to the C-terminal regions. Chimera expression detected with anti-YFP antibody was similar to STIM1 or STIM2 (Fig. 2*K*).

Based on this information, we examined expression, organization, and function of the C-terminal domains of both STIM1 and STIM2 (Fig. 1*B*) expressed as C-terminally labeled YFP-fusion constructs (S1ct–YFP and S2ct–YFP). Both proteins could be expressed in HEK–Orai cells (Fig. 3*A Upper*) and were uniformly distributed in the cytoplasm (see Fig. 4). HEK–Orai cells transfected with S1ct–YFP had significant constitutive Ca^{2+} entry and a large, rapid increase in Ca^{2+} entry upon application of 50 μM 2-APB (Fig. 3*B*), which was surprising considering the lack of 2-APB effect on full-length STIM1 (Fig. 2*A*). Electrophysiological measurements in HEK–Orai1 cells revealed S1ct–YFP induced a constitutive Ca^{2+} current of ≈2 pA/pF, rapidly elevated up to ≈15 pA/pF with 50 μM 2-APB (Fig. 3*C*). The inwardly rectifying *I/V* curve (Fig. 3*D*) revealed the currents were exclusively CRAC-like. Previous studies also reported constitutive coupling between C-terminal STIM1 and Orai1 (24, 29, 30) with a similar basal current of ≈3–4 pA/pF (24, 30). S2ct–YFP expressed in HEK–Orai1 cells also caused constitutive Ca^{2+} entry and 2-APB-induced Ca^{2+} entry. However, the number of viable cells expressing S2ct–YFP was lower. This result may reflect toxicity from high Ca^{2+} entry because lowering external Ca^{2+} after transfection to 0.3 mM with EGTA resulted in more cells with visible fluorescence. However, only ≈20% of such transfected cells had fluorescence comparable to the brightness of the majority of S1ct–YFP-expressing cells. The current trace shown in Fig. 3*E* is from one of these brighter S2ct–YFP-transfected cells and revealed constitutive Ca^{2+} current of 3 pA/pF and a huge 2-APB-induced current peaking at almost 100 pA/pF (Fig. 3*E*). Thus, S2ct–YFP cells of comparable YFP intensity had similar constitutive I_{CRAC} but much greater 2-APB-induced I_{CRAC} than for S1ct–YFP, indicating S2ct may have a more efficient 2-APB-activated coupling.

We sought to further functionally dissect the STIM1 C-terminal domain. Previous studies suggested the lysine-rich end of the C-terminal STIM1 domain is important for anchoring and/or facilitating the coupling to activate Orai channels (29, 30). Expression of the STIM1 C terminus devoid of the 672-685 K-rich sequence (S1ctΔK; see Fig. 1*B*) resulted in similar activation of Ca^{2+} entry in HEK–Orai1 cells (Fig. 3*F*). Elimination of all but the coiled-coil region of STIM1 (S1ctCC; see Fig. 1*B*) again gave rise to Ca^{2+} entry (Fig. 3*G*). Expression of fragments was similar to that

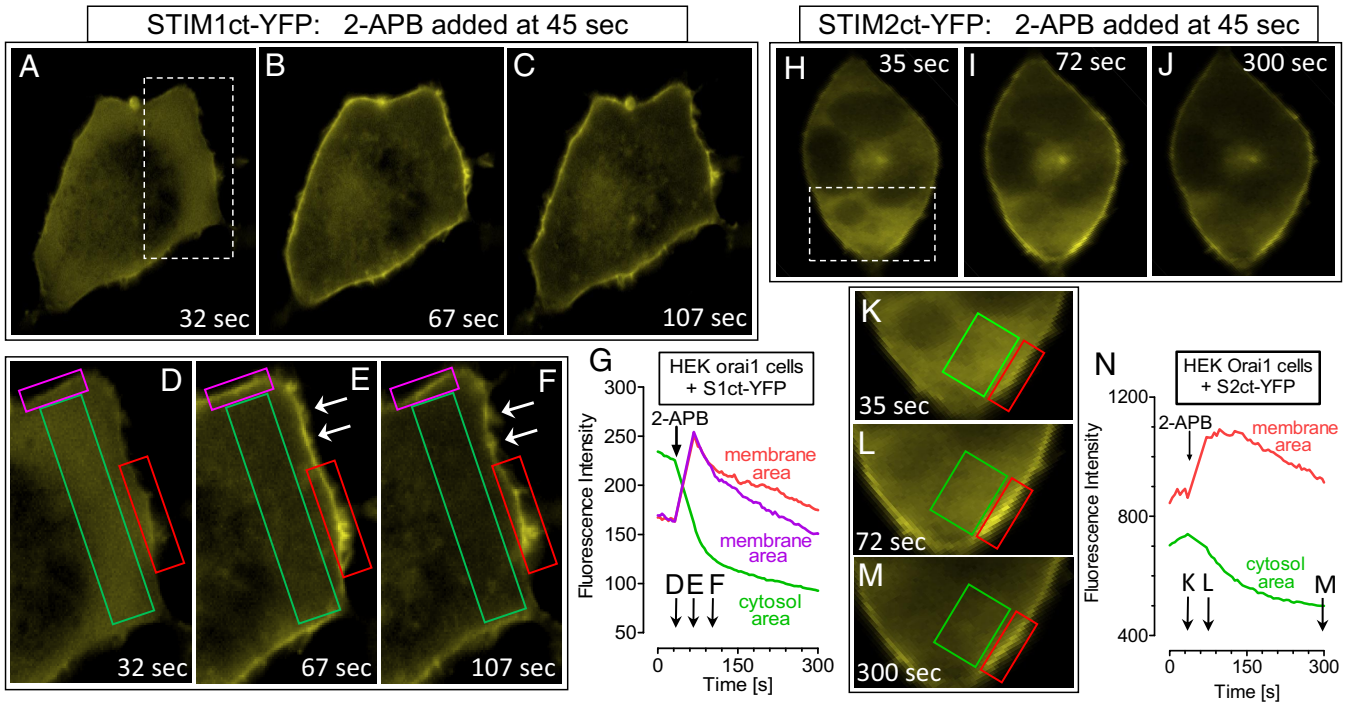

Fig. 4. Rapid cytosolic clearing and membrane association of STIM1 and STIM2 C-terminal YFP-tagged fragments induced by 2-APB. (*A–C*) Time course of the redistribution of S1ct–YFP fluorescence in HEK–Orai1 cells transfected with S1ct–YFP induced by 50 μM 2-APB added at 45 s. (*D–F*) Magnified detail of the boxed area shown in *A*. Note the clearing of cytosolic S1ct–YFP, its attachment to the membrane, and redistribution within the membrane at later times (arrows). (*G*) Time course of averaged changes of S1ct–YFP fluorescence in the boxed areas shown in *D–F*; membrane areas are red and purple); cytosolic area is green. Average fluorescence change in membrane and cytosol were +137 ± 33 and −104 ± 18, respectively (n = 3). (*H–J*) Time course of the redistribution of S2ct–YFP fluorescence induced by 50 μM 2-APB in HEK–Orai1, as in *A–C*. (*K–M*) Time course of redistribution of S2ct–YFP fluorescence in boxed area shown in *I*. (*N*) Time course of averaged changes of S2ct–YFP fluorescence of membrane (red) and cytosolic (green) areas in the boxed regions in *K–M*. Average fluorescence change in membrane and cytosol were +147 ± 42 and −82 ± 21, respectively (n = 3). (Magnifications: ×3,000.)

of the complete C termini (Fig. 3*A*). In both cases, the truncation reduced the 2-APB component rather than the constitutive component of Ca^{2+} entry.

Important to assess was whether the STIM1 C-terminal fragment acts directly on Orai1 or requires endogenous STIM proteins to mediate coupling. Clearly, the S1ct–YFP construct expressed in DT40–S1/S2$^{-/-}$ cells was highly active, with a rapid and large 2-APB-induced Ca^{2+} entry (Fig. 3*H*). The S1ct also does not require exogenously expressed Orai1-activating endogenous Orai channels (Orai1 and Orai2 in DT40 cells); overexpression of Orai1–CFP had a minimal effect (Fig. 2*I*). Interestingly, there was no S1ct-induced constitutive Ca^{2+} entry in the S1/S2$^{-/-}$ DT40 cells, whereas in wt-DT40 cells S1ct resulted in significant constitutive Ca^{2+} entry (data not shown), which indicates that S1ct-induced constitutive entry and 2-APB-dependent entry are distinct events. Another difference in DT40 cells is the prolonged entry activated by S1ct (Fig. 3 *H* and *I*); however, removal of external Ca^{2+} resulted in slowly decreasing Ca^{2+} (data not shown), thus, compared with HEK cells DT40 cells appear to have lower Ca^{2+} pumping activity.

Clearly, the cytoplasmic S1ct becomes functionally coupled by 2-APB to profoundly activate Orai1 channels. We next addressed whether this activation represented a physical relocation of the S1ct protein. With HEK–Orai cells, imaging revealed S1ct-YFP to be relatively evenly distributed within the cytosol (Fig. 4*A*). Just 20 s after the addition of 50 μM 2-APB, much S1ct became attached to the PM and much had cleared from the cytosol (Fig. 4*B*), a process that continued over the subsequent 40 s (Fig. 4*C*). High-resolution details of this movement (Fig. 4 *D–F*) revealed not only the 2-APB-induced cytosolic clearing and membrane-association of S1ct, but also a significant change in the local organization of S1ct after its attachment to the membrane (arrows in Fig. 4 *E* and *F*). The kinetics of changes of fluorescence intensity in the cytosol and PM areas (Fig. 4*G*) match well with each other with the rate of activation of Ca^{2+} entry and CRAC channels shown in Fig. 3. The distribution and 2-APB-induced redistribution of S2ct–YFP (Fig. 4 *H–N*) were essentially the same as for S1ct–YFP. In HEK293 cells not overexpressing Orai1, there were only very small 2-APB-induced changes in the distribution of expressed S1ct–YFP and S2ct–YFP (data not shown). Therefore, the redistribution of the C-terminal STIM fragments is an Orai1-mediated event.

Last, we examined the association and interaction of C-terminal STIM fragments with the Orai1–CFP protein in HEK–Orai cells expressing both proteins. The stably expressed Orai1–CFP protein was exclusively and relatively uniformly located in the PM (Fig. 5*A*). Before 2-APB addition, S1ct–YFP was uniformly cytoplasmic in the same cell (Fig. 5*B*). Interestingly, 20 s after 50 μM 2-APB addition, Orai1–CFP had undergone considerable reorganization into discrete areas in the PM (Fig. 5*C*), and at the same time S1ct–YFP had become associated with and organized within the same areas (Fig. 5*D*). Magnifications of these events in the same cell are shown in Fig. 5 *E–J*. Clearly, the areas of association and organization of Orai1–YFP and S1ct–YFP are nearly identical (Fig. 5 *H* and *I*) and the merged images before and after 2-APB (Fig. 5 *G* and *J*) reinforce the almost complete overlap of the 2 proteins. This remarkable 2-APB-induced reorganization and colocalization was also observed for S2ct–YFP coexpressed with Orai1–CFP (Fig. 5 *K–T*). Note from the magnified images for S2ct–YFP how uniformly labeled the Orai1–CFP was in the PM before 2-APB (Fig. 5 *O* and *Q*), and how the reorganization of both Orai and STIM is almost perfectly superimposed within spatially defined domains within the PM (Fig. 5 *R–T*). This same reorganization of expressed Orai1 and S1ct was also seen in DT40S1/S2$^{-/-}$ cells;

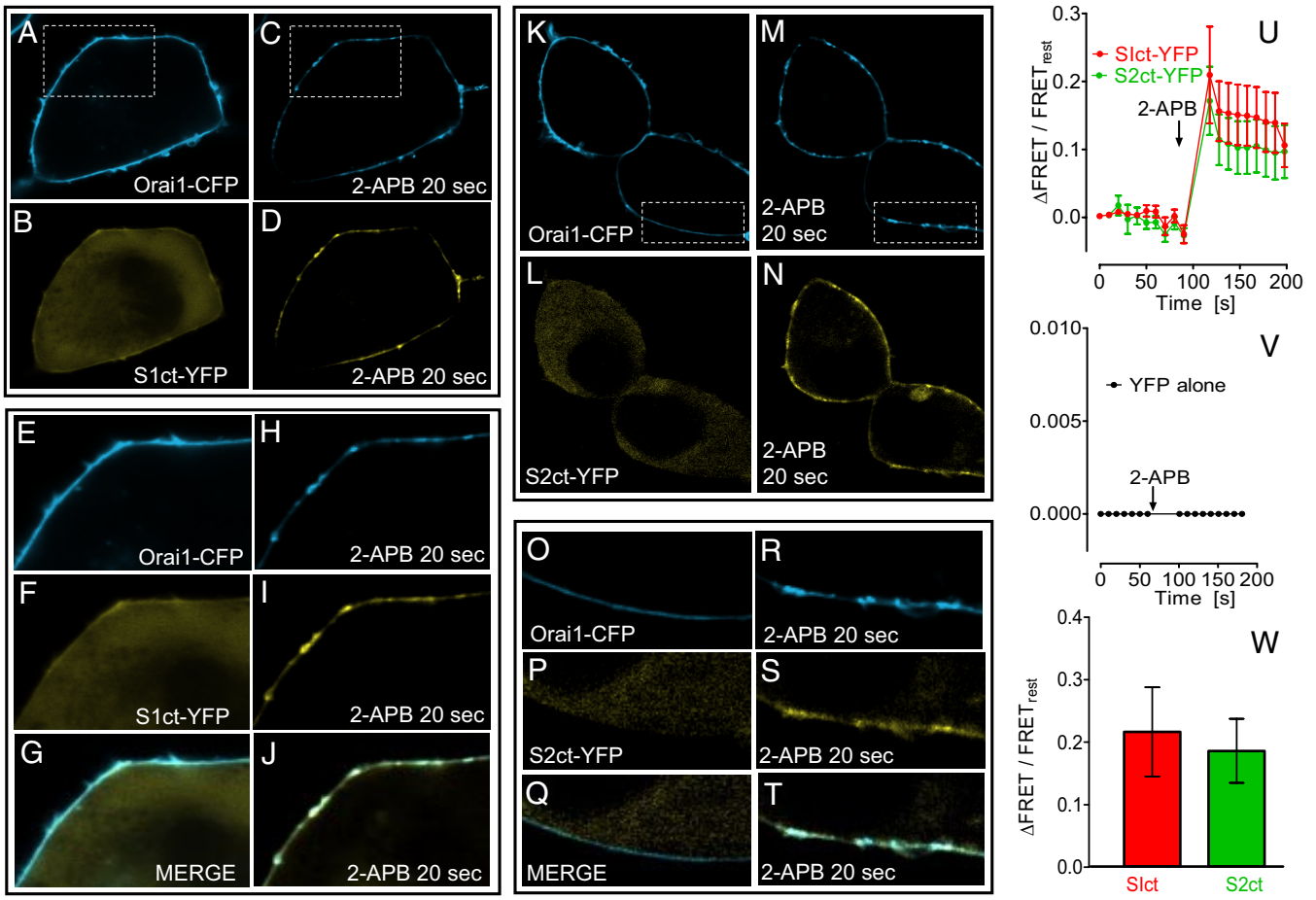

Fig. 5. Redistribution and interaction between Orai–CFP and YFP-tagged STIM1 and STIM2 C-terminal fragments induced by 2-APB. (*A–T*) Stably expressing HEK–Orai cells were transfected with either S1ct-YFP (*A–J*) or S2ct–YFP (*K–T*). (*A* and *C*) Orai–CFP fluorescence before and 20 s after 50 μM 2-APB addition. (*B* and *D*) S1ct–YFP fluorescence in the same cells. (*E–J*) Details of fluorescence changes in boxed areas in *A* and *C*) for Orai1–CFP (*E* and *H*), S1ct–YFP (*F* and *I*), and merged Orai1–CFP/S1ct–YFP fluorescence (*G* and *J*). Note the major change in Orai–CFP membrane distribution before and after 2-APB, and the exact correspondence and overlap of Orai1–CFP/S1ct–YFP seen in the merged areas after 2-APB. The images shown in *K–T* are identical experiments to *A–J* except the STIM2 C-terminal-YFP construct in HEK-Orai cells was used. Note from the detailed images how uniform Orai–CFP is in the membrane before 2-APB (*O*) and how reorganized it becomes 20 s after 2-APB (*R*); note also the profound movement of S2ct-YFP from the cytosol (*P*) to the membrane (*S*) after 2-APB addition, and the almost complete overlap of the Orai1–CFP and S1ct-YFP fluorescence in the membrane (*T*). (*U*) Two-channel FRET analysis of the time course of interactions between Orai1–CFP and either S1ct–YFP (red) or S2ct–YFP (green), induced by 50 μM 2-APB. The values are normalized for resting FRET levels before 2-APB. (*V*) Absence of FRET signal in HEK–Orai1–CFP cells expressing cytosolic YFP alone. (*W*) Average of 6 separate FRET experiments normalized to resting FRET levels for 2-APB-induced FRET increases between Orai1–CFP and S1ct–YFP (red) or S2ct–YFP (green), revealing that relative 2-APB-induced FRET changes are similar for S1ct and S2ct. (Magnifications: ×3,000.)

hence endogenous STIM proteins are not required (data not shown). Also, in cells overexpressing only Orai1–CFP and not S1ct, there was no 2-APB-induced Orai1 reorganization (data not shown), indicating the relocation depends on the S1ct–Orai complex and is not merely an alteration of Orai1 per se.

The overlap of fluorescence between Orai1 and STIM C termini indicated a close interaction. We undertook FRET measurements to gauge the proximity of interactions between the 2 proteins. As shown in Fig. 5*U*, 2-channel FRET analysis between Orai–CFP and either S1ct–YFP or S2–YFP proteins expressed exactly as in the above images, in both cases revealed a rapid 2-APB-induced increase in FRET. Because S2ct–YFP was expressed at lower levels than S1ct–YFP, the data were normalized to the level of resting FRET before 2-APB. The increased FRET signal remained relatively stable for 100 s, considerably longer than the rapid decline in current and Ca^{2+} entry that follows the initial peak (Fig. 3 *B*, *C*, and *E*). Thus, the inhibition of channel function does not result from dissociation between the proteins. In the same HEK–Orai1–CFP cells expressing YFP alone, there was no resting FRET or 2-APB-induced change in FRET (Fig. 5*V*). The normalized 2-APB-induced FRET changes for S1ct and S2ct were not significantly different (Fig. 5*W*).

These results provide important information on the functional coupling between STIM and Orai proteins. 2-APB is a powerful modifier of SOC function (16, 19–26), and we reveal here that 2-APB induces rapid, profound, and either direct or very close interactions between the STIM and Orai proteins, locking the C terminus of STIM proteins together with Orai1 to facilitate complete functional channel coupling. We show that just the C-terminal coiled-coil domain of STIM proteins is sufficient for Orai1 activation. Thus, 2-APB appears to bypass and substitute for the elaborate multimerization and reorganization of STIM that is considered a prerequisite for Orai channel activation (31, 32). Indeed, we show that the functional STIM–Orai coupling mediated by 2-APB has no requirement for endogenous ER STIM proteins because the same rapid functional coupling can occur in DT40S1/S2$^{-/-}$ cells.

The results also reveal a surprising reorganization of Orai1 channels rapidly occurring in the PM during the STIMct-dependent, 2-APB-induced activation process. Until now reorganization of Orai in the PM has been considered dependent only on

capture within PM regions juxtaposed with ER puncta containing STIM (31, 32). Our results suggest that the Orai–STIMct complex has an intrinsic ability to cluster in the PM. We do not yet know whether the Orai–STIMct aggregates we observe are related to channel activation, or if they reflect the inactivation of channels that rapidly follows 2-APB-induced activation. Aggregation of Orai1 into μm-sized clusters in the PM was recently reported to occur through altered electrostatic interactions of acidic residues in the Orai1 C terminus (33), possibly mediated by the STIMct. Whereas 2-APB causes a massive association between STIMct and Orai1, some constitutive association between STIMct and Orai1 can occur without 2-APB, a result agreeing with 3 recent reports in which STIM1ct was examined (24, 30, 34). Clearly, a small amount of S1ct is constitutively bound to Orai1 in the membrane (see Fig. 5 *B* and *F*), but there is no evidence of spatial organization of Orai1 without 2-APB, a result also noted by others (30, 34). We also observe no changes of 2-APB on endogenous STIM1 puncta formation. In contrast, 2-APB was reported to prevent STIM1 puncta (22, 25), although a recent study revealed this effect occurs only with extended 2-APB exposure (35). Importantly, in the same study, FRET analysis between coexpressed full-length STIM1 and Orai1 revealed that 50 μM 2-APB could induce an increased association between the proteins after store depletion, but it did not visibly alter STIM1 or Orai1 in puncta.

We reveal that both STIM1ct and STIM2ct can activate Orai1 channels. The greater effectiveness of endogenous STIM2 likely reflects a combination of increased N-terminal sensitivity to changes in ER Ca^{2+} (13) and a greater effectiveness of 2-APB in promoting the C terminus to activate Orai1 channels. Whereas the rapid and large activation of Orai1 by 2-APB requires the presence of STIM1ct or STIM2ct, in contrast, we provide definitive proof that Orai3 can be activated by 2-APB independently of both STIM1 and STIM2. We speculate that 2-APB may bind to similar sites on both Orai proteins, for Orai1, enhancing conformational coupling with STIM1 to activate current, and for Orai3, perhaps substituting for the STIM-binding requirement for current activation. However, the massive STIM1-dependent activation of Orai1 by 2-APB does not change its ion selectivity properties (Figs. 2*C* and 3*D*), whereas 2-APB curiously changes Orai3 ion selectivity (22–25).

Overall, in addition to defining a clear action of 2-APB in locking STIMct with Orai1, the results reveal that this coupling involves a profound and intimate correspondence between STIMct-binding, transient Orai1 channel activation, and relocation of the entire complex within the PM. Moreover, the locked STIMct–Orai complex may provides a useful stable system with which to structurally probe the sites of interaction between STIM and Orai proteins.

Methods

DNA Constructs, Cell Culture, and Transfection. Fluorescent STIM1, STIM2, and Orai1 constructs were all inserted in the pIRESneo plasmid (Clontech). CFP-tagged Orai2 and Orai3 were kindly donated by James Putney Jr. (National Institute of Environmental Health Sciences, Triangle Park, NC). S1ct and S2ct were generated by truncation of the 1M-234N segment of STIM1–YFP and 1L-238N segment of STIM2–YFP, respectively. S1ctΔK and S1ctCC were generated by C-terminal truncations of the C-terminal portions of S1ct (667S-685K and 506P-685K, respectively). S1/S2 chimeras were generated by single-point fusions of the extracellular/luminal portion of STIM1 (1M-201P) with the transmembrane and cytoplasmic regions of STIM2 (206L-746). HEK293 cells and chicken DT40 cells were maintained as described (14, 16). HEK293 cells stably expressing Orai1–CFP (HEK–Orai cells) were generated by electroporation of the Orai1–pIRES construct and selection as described (36). KO DT40 cells were gifts from Tomohiro Kurosaki (RIKEN). $S1^{-/-}$, $S2^{-/-}$, and $S1/S2^{-/-}$ DT40 cells were generated as described by Baba et al. (37). Transfection of DNA into cells was achieved by electroporation by using the BioRad Xcel electroporation system as described (14).

Other Methods. A summary of methodology for measurements of intracellular Ca^{2+}, electrophysiology, Western analysis, fluorescence imaging, and FRET is provided in *SI Text*.

ACKNOWLEDGMENTS. This work was supported by National Institutes of Health Grant AI058173 (to D.L.G.), and the American Heart Association (J.S.).

1. Lewis RS (2007) The molecular choreography of a store-operated calcium channel. *Nature* 446:284–287.
2. Hogan PG, Rao A (2007) Dissecting I CRAC, a store-operated calcium current. *Trends Biochem Sci* 32:235–245.
3. Hewavitharana T, Deng X, Soboloff J, Gill DL (2007) Role of STIM and Orai proteins in the store-operated calcium signaling pathway. *Cell Calcium* 42:173–182.
4. Roos J, et al. (2005) STIM1, an essential and conserved component of store-operated Ca^{2+} channel function. *J Cell Biol* 169:435–445.
5. Liou J, et al. (2005) STIM is a Ca^{2+} sensor essential for Ca^{2+} -store-depletion-triggered Ca^{2+} influx. *Curr Biol* 15:1235–1241.
6. Spassova MA, et al. (2006) STIM1 has a plasma membrane role in the activation of store-operated Ca^{2+} channels. *Proc Natl Acad Sci USA* 103:4040–4045.
7. Zhang SL, et al. (2005) STIM1 is a Ca^{2+} sensor that activates CRAC channels and migrates from the Ca^{2+} store to the plasma membrane. *Nature* 437:902–905.
8. Feske S, et al. (2006) A mutation in Orai1 causes immune deficiency by abrogating CRAC channel function. *Nature* 441:179–185.
9. Vig M, et al. (2006) CRACM1 is a plasma membrane protein essential for store-operated Ca^{2+} entry. *Science* 312:1220–1223.
10. Zhang SL, et al. (2006) Genomewide RNAi screen of Ca^{2+} influx identifies genes that regulate Ca^{2+} release-activated Ca^{2+} channel activity. *Proc Natl Acad Sci USA* 103:9357–9362.
11. Venkatachalam K, van Rossum DB, Patterson RL, Ma HT, Gill DL (2002) The cellular and molecular basis of store-operated calcium entry. *Nat Cell Biol* 4:E263–E272.
12. Parekh AB, Putney JW, Jr (2005) Store-operated calcium channels. *Physiol Rev* 85:757–810.
13. Brandman O, Liou J, Park WS, Meyer T (2007) STIM2 is a feedback regulator that stabilizes basal cytosolic and endoplasmic reticulum Ca^{2+} levels. *Cell* 131:1327–1339.
14. Hewavitharana T, et al. (2008) Location and function of STIM1 in the activation of Ca^{2+} entry signals. *J Biol Chem* 283:26252–26262.
15. Peinelt C, et al. (2006) Amplification of CRAC current by STIM1 and CRACM1 (Orai1). *Nat Cell Biol* 8:771–773.
16. Soboloff J, et al. (2006) Orai1 and STIM reconstitute store-operated calcium channel function. *J Biol Chem* 281:20661–20665.
17. Mercer JC, et al. (2006) Large store-operated calcium-selective currents due to coexpression of Orai1 or Orai2 with the intracellular calcium sensor, Stim1. *J Biol Chem* 281:24979–24990.
18. Wu MM, Buchanan J, Luik RM, Lewis RS (2006) Ca^{2+} store depletion causes STIM1 to accumulate in ER regions closely associated with the plasma membrane. *J Cell Biol* 174:803–813.
19. Ma HT, et al. (2000) Requirement of the inositol trisphosphate receptor for activation of store-operated Ca^{2+} channels. *Science* 287:1647–1651.
20. Prakriya M, Lewis RS (2001) Potentiation and inhibition of Ca^{2+} release-activated Ca^{2+} channels by 2-aminoethyldiphenyl borate (2-APB) occurs independently of IP 3 receptors. *J Physiol* 536:3–19.
21. Ma HT, Venkatachalam K, Parys JB, Gill DL (2002) Modification of store-operated channel coupling and inositol trisphosphate receptor function by 2-aminoethoxydiphenyl borate in DT40 lymphocytes. *J Biol Chem* 277:6915–6922.
22. Dehaven WI, Smyth JT, Boyles RR, Bird GS, Putney JW, Jr (2008) Complex actions of 2-aminoethyldiphenyl borate on store-operated calcium entry. *J Biol Chem* 283:19265–19273.
23. Schindl R, et al. (2008) 2-Aminoethoxydiphenyl borate alters selectivity of orai3 channels by increasing their pore size. *J Biol Chem* 283:20261–20267.
24. Zhang SL, et al. (2008) Store-dependent and -independent modes regulating Ca^{2+} release-activated Ca^{2+} channel activity of human Orai1 and Orai3. *J Biol Chem* 283:17662–17671.
25. Peinelt C, Lis A, Beck A, Fleig A, Penner R (2008) 2-Aminoethoxydiphenyl borate directly facilitates and indirectly inhibits STIM1-dependent gating of CRAC channels. *J Physiol (London)* 586:3061–3073.
26. Parvez S, et al. (2007) STIM2 protein mediates distinct store-dependent and store-independent modes of CRAC channel activation. *FASEB J* 22:752–761.
27. Stathopulos PB, Zheng L, Li GY, Plevin MJ, Ikura M (2008) Structural and mechanistic insights into STIM1-mediated initiation of store-operated calcium entry. *Cell* 135:110–122.
28. Stathopulos PB, Zheng L, Ikura M (2008) Stromal interaction molecule (STIM)1 and STIM2 EF-SAM regions exhibit distinct unfolding and oligomerization kinetics. *J Biol Chem* 284:728–732.
29. Huang GN, et al. (2006) STIM1 carboxyl-terminus activates native SOC, I(crac) and TRPC1 channels. *Nat Cell Biol* 8:1003–1010.
30. Muik M, et al. (2008) Dynamic coupling of the putative coiled-coil domain of ORAI1 with STIM1 mediates ORAI1 channel activation. *J Biol Chem* 283:8014–8022.
31. Luik RM, Wu MM, Buchanan J, Lewis RS (2006) The elementary unit of store-operated Ca^{2+} entry: Local activation of CRAC channels by STIM1 at ER-plasma membrane junctions. *J Cell Biol* 174:815–825.
32. Luik RM, Wang B, Prakriya M, Wu MM, Lewis RS (2008) Oligomerization of STIM1 couples ER calcium depletion to CRAC channel activation. *Nature* 454:538–542.
33. Calloway N, Vig M, Kinet JP, Holowka D, Baird B (2008) Molecular clustering of STIM1 with Orai1/CRACM1 at the plasma membrane depends dynamically on depletion of Ca^{2+} stores and on electrostatic interactions. *Mol Biol Cell* 20:389–399.
34. Penna A, et al. (2008) The CRAC channel consists of a tetramer formed by Stim-induced dimerization of Orai dimers. *Nature* 456:116–120.
35. Navarro-Borelly L, et al. (2008) STIM1–ORAI1 interactions and ORAI1 conformational changes revealed by live-cell FRET microscopy. *J Physiol (London)* 586:5383–5401.
36. Soboloff J, et al. (2006) STIM2 is an inhibitor of STIM1-mediated store-operated Ca^{2+} entry. *Curr Biol* 16:1465–1470.
37. Baba Y, et al. (2006) Coupling of STIM1 to store-operated Ca^{2+} entry through its constitutive and inducible movement in the endoplasmic reticulum. *Proc Natl Acad Sci USA* 103:16704–16709.
38. Soboloff J, et al. (2005) Role of endogenous TRPC6 channels in Ca^{2+} signal generation in A7r5 smooth muscle cells. *J Biol Chem* 280:39786–39794.